MODELING OF DRYING PROCESS IN A PNEUMATIC CONVEYOR: PART I - FLUID DYNAMIC ANALYSIS

Maria do Carmo Ferreira
Chemical Engineering Department- Federal University of São Carlos – P.O. Box 676 – 13565-905 - São Carlos - SP
mariaf@power.ufscar.br

José Teixeira Freire
Chemical Engineering Department- Federal University of São Carlos – P.O. Box 676 – 13565-905 - São Carlos - SP
freire@power.ufscar.br

Abstract. *Aiming a further automation of a pneumatic conveyor dryer, the purpose of this work is to analyze the modeling of the drying process in a pneumatic conveyor. The analysis was performed by simulating the fluid dynamics behavior of gas-solid flow in a vertical duct. The two-fluid one-dimensional model has been applied to describe the flow. Four equations of momentum and mass balances for the solid and fluid phases were numerically solved to provide estimates of the flow pressures, voidages and phase velocities along the tube. An analysis of the physical consistency of the equations and of the simplifying assumptions adopted was presented, considering aspects such as the smallest representative control volume and the use of Eulerian approach to model the solid phase as a continuous fluid. The results obtained by the simulations were compared with experimental data in order to check the performance of the equations for predicting the fluid dynamic variables and the expected behaviors in gas-solid flow. The results show that the model is successful in predicting variables such as the pressure gradients at dilute flow for different ranges of operational conditions. The model can also provide good estimates of the transition velocity between dilute and dense-phase transport, as well of the entrance length.*

Keywords*. Two fluid one-dimensional model, pressure gradients, entrance length, transition velocity.*

1. Introduction

Pneumatic conveyors are often applied in drying operations, particularly for drying of food granules and powders that require low residence times in contact with a high temperature fluid. An important aspect to be considered in the design and operation of food drying equipment is the necessity of preserving the quality and characteristics of the original material. In pneumatic transport the particles are conveyed by a heated air stream in a vertical duct, being continuously dried. During the process, several parameters need to be carefully controlled in order to ensure the product quality. Because the materials are thermal sensible, the air flow rates must be high enough to ensure very low residence times, the air temperatures cannot reach extremely high values in order to avoid product degradation and the moisture content in the final product must be reduced until the recommended value for stocking purposes (usually lower than 3%). The use of automation and on-line control in such kind of operation is not widespread yet, but with the recent developments in such techniques, they appear as promising alternatives for process optimization and improving of product quality. A reliable model to describe the complex problem of coupled mass, momentum and energy transfer involved in the drying process is essential for implementation of automation and control systems. In spite of being representative, the model must be simple enough to allow fast responses from the system when corrective actions are required to keep the stipulated values of the controlled variables.

The interactions between a discrete particulate-phase with a continuous fluid in a turbulent flow is characterized by complex physical phenomena acting simultaneously on the boundary layers developed around the solids (Berker, 1963; Clift et al., 1979). A detailed simulation aiming the prediction of local variables, such as the particle and fluid velocities and local particle concentration may become a very complicated task. The modeling of particulate two-phase flow is usually performed by using either a Lagrangian model or a Eulerian approach. In the first case, the particles are modeled as a discrete phase and the motion of solids, as well as the collision effects are predicted by solving the Newtonian equations of motion for each suspended solid particle (Hoomans et al., 1996; Huber and Sommerfield, 1998; Ouyang and Li, 1999). The fluid motion and effects of turbulence are considered by the conservation equations applied to the continuous fluid phase. In the Eulerian approach, both the particles and the fluid are considered to be continuous and are described in terms of separate sets of conservation equations with appropriate interaction terms representing the coupling between the two phases (Gidaspow, 1994; Niewland et al., 1996; Enwald and Almstedt, 1999; Levy, 2000). Whatever approach is adopted, specification of the proper initial and boundary conditions are required.

The choice of the model depends primarily on what kind of application the simulation will be used for. In the Lagrangian approach, a direct solution of the whole set of conservation equations requires powerful computational tools and the number of particles in the flow may be a limiting aspect to be considered (Graham and Moyeed, 2002). All the forces affecting the flow, such as drag, centrifugal and lift forces may be incorporated into the model and the particle´s trajectories can be estimated at every position. The model validation, however, requires detailed measurements of local variables for each phase, and is often difficult to be performed.

On the other hand, the two-fluid models obtained from the Eulerian approach cannot recognize the discrete character of the solid phase. The resulting equations are usually simpler to be solved than those obtained from the Lagrangian approach. In spite of all the simplifying assumptions, a great number of authors has been successfully applying two-fluid models to understand the physics underlying two-phase flow systems, such as in fluidized beds (Gidaspow, 1986; Kuipers et al., 1992; Boemer et al., 1995; Enwald et al., 1996). The equations representing the Eulerian model contain empirical submodels and, thus, a procedure to compare the solution from the model with experimental data is required. The model validation in this case is facilitated because the measured variables are those from the gas-solid mixture.

Aiming a further automation of a pneumatic conveyor dryer, the purpose of this work is to analyze the modeling of the drying process in a pneumatic conveyor. The analysis will be performed by initially simulating the fluid dynamics behavior of gas-solid flow in a vertical duct. The one-dimensional two-fluid model will be applied to describe the flow (Soo, 1967; Capes and Nakamura, 1973; Deich et al., 1974; Arastoopour and Gidaspow, 1979; Telles and Massarani, 1980). In this model, four equations of momentum and mass balances for the solid and fluid phases are considered. The equations will be solved in order to provide predictions of flow pressure, voidage and phase velocities along the tube. An analysis of the physical consistency of equations and of the simplifying assumptions adopted will be carried out, considering aspects such as the smallest representative control volume and the use of Eulerian approach to model the solid phase as a continuous fluid. The results obtained by the simulation will be compared with experimental data in order to check the performance of the equations for predicting the fluid dynamic variables and expected behaviors in gas-solid flow.

2. Fluid Dynamics Equations

In steady state flow, the continuity equations for the gas and solid phases can be written as:

$$\frac{d}{dz}(\rho_f\ v_f\,\varepsilon) = 0 \tag{1}$$

$$\frac{d}{dz}[(\rho_s v_s (1-\varepsilon)] = 0 \tag{2}$$

In these equations, ρ_f and ρ_s are the fluid and particle densities, v_f and v_s are the fluid and particle interstitial velocities, ε is the volumetric mean voidage, defined as the relationship between the volume occupied by the fluid phase and the volume of transport tube and z is the flow direction.

The transport momentum equations may differ depending on the simplifications adopted by each author. A summary of the most common equations applied to vertical gas-solid flow is given in Table (1). In Equations (3) to (11), P is the pressure, g is the gravitational acceleration, F_d is the gas-fluid drag force, F_f and F_p is the wall-friction forces for the gas and particles, respectively.

In the model proposed by Soo (1967), the pressure gradient is considered only in the equation for the fluid-phase. A drag force was included to consider the interaction between the solid and the fluid phases. In the uniform flow model proposed by Capes and Nakamura (1973) similar equations are written for each phase. It is assumed a partial pressure gradient acting in each phase and the contribution of each phase to the total pressure gradient is considered to be proportional to the volume fraction occupied by the phase in the transport tube. The volumetric mean voidage, ε, is used to define the volume fraction of each phase. Empirical equations must be provided for the fluid-dynamic drag force and for the wall friction terms, F_f and F_p. Deich et al. (1974) adopted the momentum equation for the gas-solid mixture and also considered a pressure gradient acting in the solid phase, corrected by the volumetric voidage. These two last authors did not consider the presence of wall-friction forces. Arastoopour and Gidaspow (1979) proposed an equation for the solid-phase that is based on the slip velocity between the phases, and a momentum equation written for the gas-solid mixture. They consider a term for the fluid-wall friction force, but the solid-wall friction force was neglected and only the drag force appears on the solid-phase momentum equation. Telles and Massarani (1980) proposed the use of equations for the fluid and solid phases, and the interaction between the phases are accounted by a resistive force, m, which must be determined empirically. This model was applied for both pneumatic and hydraulic conveying. In this later case, the empirical equations for the resistive force were obtained by Massarani and Santana (1994) from fluidization experiments.

The system of four equations composed by the continuity and the momentum equations can be solved simultaneously by numerical integration on the axial direction, providing estimates of voidage, pressure, gas velocity and solid velocity as functions of the tube length. One of the difficulties in solving this system is the need of reliable constitutive equations for estimating the interaction forces: the drag or resistive force between fluid and solids and the wall friction forces. The wall friction forces for the fluid and particulate phases (F_f and F_p) are usually written in terms of fluid-wall and particle-wall friction coefficients, f_f and f_p, assuming that the Fanning equation classically employed for a continuous phase can be also applied for the particulate phase, so:

$$F_f = \frac{2 f_f \varepsilon \rho_f\ v_f^{\,2}}{D_t} \tag{13}$$

$$F_p = \frac{2f_p(1-\varepsilon)\rho_p\, v_s^{\,2}}{D_t} \tag{14}$$

where D_t is the transport tube diameter.

Table 1. Momentum equations on two-fluid one-dimensional models.

Author	Equations
Soo, (1967)	$(1-\varepsilon)\rho_s v_s \frac{dv_s}{dz} + \varepsilon\rho_f v_f \frac{dv_f}{dz} + (\rho_s(1-\varepsilon)+\varepsilon\rho_f)g = -\frac{dP}{dz}$ (3) $\rho_s v \frac{d\,v_s}{dz} = +F_d - \rho_s g$ (4)
Capes and Nakamura, (1973)	$\frac{d}{dz}(\rho_f \varepsilon\, v_f^{\,2}) = \varepsilon\left(-\frac{dP}{dz}\right) - \varepsilon\rho_f g - F_d - F_f$ (5) $\frac{d}{dz}[\rho_s(1-\varepsilon)\, v_s^{\,2}] = (1-\varepsilon)\left(-\frac{dP}{dz}\right) - (1-\varepsilon)\rho_s g + F_d - F_p$ (6)
Deich et al., (1974)	$(1-\varepsilon)\rho_s\ v_s \frac{d\,v_s}{dz} + \varepsilon\rho_f\ v_f \frac{d\,v_f}{dz} + (\rho_s(1-\varepsilon)+\varepsilon\rho_f)g = -\frac{dP}{dz}$ (7) $\rho_s\ v_s \frac{d\,v_s}{dz} = +\frac{P}{(1-\varepsilon)}\frac{d\varepsilon}{dz} - \frac{dP}{dz} + F_d - \rho_s g$ (8)
Arastoopour and Gidaspow, (1979)	$(1-\varepsilon)\rho_s\ v_s \frac{d\,v_s}{dz} + \varepsilon\rho_f\ v_f \frac{d\,v_f}{dz} + (\rho_s(1-\varepsilon)+\varepsilon\rho_f)g + F_f = -\frac{dP}{dz}$ (9) $-\frac{1}{2}\frac{d}{dz}(v_f - v_s)^2 = \frac{F_d}{\rho_s} - g$ (10)
Telles and Massarani, (1992)	$\rho_f \varepsilon\ v_f \frac{d\,v_f}{dz} = -\frac{dP}{dz} - \rho_f\, g - m$ (11) $(1-\varepsilon)\rho_s\ v_s \frac{d\,v_s}{dz} = -(1-\varepsilon)(\rho_s - \rho_f)g + m$ (12)

While the gas-wall friction coefficient can be easily obtained from one of the several correlations available in the literature (e.g. Blasius or Colebrook, in Bird, 2002), the same is not true of solid-wall friction coefficient. A review of some of the expressions for predicting the solid-wall friction coefficients can be found in Marcus et al. (1990). Most correlations are adjusted from measurements of pressure gradients and experimental mean voidages. Many correlations are reported, but there is a large discrepancy between the expressions, because they are strongly dependent on the flow conditions, particle characteristics and even the transport tube configuration. Some authors (Arastoopour and Gidaspow, 1979 and Littman et al., 1993) claim that the contribution of solid-wall friction forces in the momentum balance is expected to be small for dilute-phase transport. However, except by some few works that report the existence of a particle-free zone in the near wall region (Lee and Durst, 1982), there is little experimental evidence to support the generalization of such an assumption.

The drag force is normally correlated with the slip velocity through an effective drag coefficient defined for the two-phase flow using a similar concept to the classical drag coefficient defined for a single particle falling at steady state in an infinite medium. Assuming that the fluid dynamic drag force is proportional to the square of the slip velocity, a volumetric drag coefficient, β, is defined by the equation:

$$F_d = \beta(v_f - v_s)^2 \tag{15}$$

Different equations may be used to relate β and the standard drag coefficient, defined for the falling of a single spherical particle, C_{ds}. Gidaspow (1994), proposed the use of following expression:

$$\beta = \frac{3}{4} C_{ds} \frac{\varepsilon\left|v_f - v_s\right|\rho_f(1-\varepsilon)}{d_p}\varepsilon^{-2.65} \tag{16}$$

The values of C_{ds} are obtained from one of the many empirical correlations available in literature for spherical particles. The expressions are functions of the particle Reynolds, Re_p. Some equations are presented in Table (2).

Table 2. – Empirical equations for C_{ds}

Author	Equation
Rowe, (1961).	$C_{ds} = 0.44$, $Re_p >= 1000$ (17) $C_{ds} = \frac{24}{Re_p}\left(1+0.15\,Re_p^{0.687}\right)$, $Re_p < 1000$ (18)
Khan and Richardson, (1987)	$C_{ds} = \left(2.25\,Re_p^{-0.31}+0.36\,Re_p^{0.06}\right)^{3.45}$,$Re_p<3x10^5$ (19)
Haider and Levenspiel, (1989)	$C_d = \frac{24}{Re_p}\left(1+0.1806\,Re_p^{0.6459}\right)+\frac{0.4251}{1+\frac{6880.95}{Re_p}}$,$Re_p<2.6x10^5$ (20)

An alternative approach to estimate the drag forces is the use of empirical correlations for the slip velocities, such as the one defined by Richardson-Zaki (1954) for liquid fluidized systems and sedimentation. Although the use of Richardson-Zaki relationship is often extended for pneumatic transport (Capes and Nakamura, 1973), its application for gas-solid mixtures with mean voidages usually greater than 0.95 is doubtful, since it was not adjusted for this range of voidages.

3. Results

3.1. Physical analysis of the two-fluid model

A consistent formulation for the problem of two-phase flow through a pipe of constant diameter D and length L, for the situation in which both fluids are continuous, is presented by Bird et al. (2002). The authors assume that a shear stress acts on the fluids interface. A pressure drop is established in the flow and defines a pressure gradient, $(P_L\text{-}P_0)/L$ which represents the flow driving force for both phases. In the two-fluid model, basically the same formulation is applied to the gas-solid flow through a pipe, assuming that both the gas and the particles behave as continuous fluids and are homogeneously distributed over the cross section of the transport tube. The conservation of mass and momentum may be applied for each phase for a control volume which is a tube section of diameter D and length Δz, leading to the two continuity equations written for each phase, Eqs. (1) and (2), and to the two momentum equations, in which are included the forces acting on an individual phase, such as in Eqs. (5) and (6), for instance. The voidage, ε, represents the volume fraction occupied by the gas and $(1\text{-}\varepsilon)$ is the volume fraction occupied by the particles in the tube.

The concept of a continuous fluid assumes that a control volume of dimension ΔV contains a sufficient number of molecules to make statistical averages meaningful for the macroscopic properties that are being considered (such as density, velocity, pressure, etc.). The value of a property at a particular point of the fluid is mathematically defined as being the function limit when $\Delta V \rightarrow 0$, with ΔV being the smallest volume surrounding the point for which statistical averages of this property are meaningful. While for a pure fluid this condition is easily satisfied by choosing a length Δz significantly larger than the mean free paths of fluid molecules, for a dispersed phase it is not well defined. According to Drew (1983), a two-phase system is characterized when a volume is occupied by two distinct materials, with different individual properties. The mixture average properties wold be a result from the partial contribution of each phase. Considering a gas-solid flow, for a control volume to be representative of the whole gas-solid mixture behavior, it should include a significant number of particles. In this case, this requirement is hardly accomplished by choosing a volume with an infinitesimal length Δz, because even a single particle has macroscopic dimension. For a two-phase system constituted by a fluid and particles, the limit $\Delta V \rightarrow 0$ must be replaced by a new definition of $\Delta V \rightarrow \Delta V_0$, where ΔV_0 is the smallest volume with meaningful and representative average properties for this system (for a detailed analyis of representative control volumes for porous systems, see Bear, 1972). So, where the momentum equations written for the fluid and the mixture are well defined and accepted by all the authors, the momentum equation for particulate phase is controversial, and the resulting equation is often modified by the authors leading to different mathematical formulations for a single physical model.

The contribution of each phase to the average properties of the mixture is another point to be analyzed. The driving force for transporting the phases is the total pressure gradient, dP/dz, which can be obtained from measurements of static pressures along the transport tube. For dilute pneumatic conveying, where usually $\varepsilon>0.95$, an analysis of the magnitude of the pressure gradients and voidages indicates that:

$$\frac{dP}{dz} \approx 1; \quad \varepsilon \approx 1 \quad \text{and} \quad (1-\varepsilon) \approx \delta \quad \Rightarrow \quad \varepsilon\frac{dP}{dz} \approx 1 \quad \text{and} \quad (1-\varepsilon)\frac{dP}{dz} \approx \delta$$

Considering the contribution of each phase to the total pressure gradient, an analysis of magnitudes indicates that for high voidages, the pressure gradient of the solid phase is very small as compared to the contribution of the fluid phase, so it is the continuous phase that really defines the mixture behavior, which explains the good predictions obtained for macroscopic variables with this model. The pressure gradient in the solid-phase equation may be considered as only a closure term for the balance, with few physical meaning.

The neglecting of the solid-wall friction force in the solid-phase momentum balance may also be justified by this analysis, since the signficance of this term is doubtful considering the small volume fractions occupied by the solids phase. Littman et al (1993) investigated the conveying of 1.0 mm glass spheres in a 28.5 mm transport tube. Based on prior evidence provided by other authors, they claimed that the contribution of F_p fraction on the total pressure gradient was expected to be much less than 8% in their system, so they neglected this term in their flow modeling. This assumption is not supported by authors who estimated the friction forces based on experimental measurements of pressure gradients and voidages. As an example, Ferreira (1996) investigated the conveying of 1.00 mm particles in a 53.0 mm transport tube and estimated solid wall friction forces from experimental measurements of voidages and pressure gradients at different experimental conditions. Comparing the fraction of the total pressure gradient consumed by each force, the author observed that the solid-wa ll friction force may be responsible for up to 60% of the total pressure drop, depending on the operational conditions, even with the experimental voidages being always greater than 0.97. Considering the lack of physical evidence to justify the high values of F_p, the author suggested that including this force in the solid-phase momentum equation might be only a form to fit the results to the experimental measurements. It must be noted also that radial variations of particle and air velocities, voidage or pressure are not considered in the one-dimensional model. The use of averaged cross-section values to estimate the slip velocities and voidages employed in the adjustement of empirical equations for F_p is a simplification and may not be representative of the whole system, introducing errors in the prediction of the solid-wall friction forces.

The two-fluid one-dimensional model cannot be considered a phenomenological model, essentially because the assumption that the particulate phase can be treated as a continuous fluid has no physical meaning. In spite of its deficiencies, the two-fluid model its simplicity make it rather attractive for predictions of macroscopic variables, such as the pressure gradient or the mean voidage and it also allows the prediction of flow regime transitions, effects of variation in the operational conditions and other relevant information from a technological point of view. Since we are interested in a simple, yet representative model for prediction of controlable variables, this model was selected to be investigated here by comparing predicted and measured values of the main variables recquired to caracterize the gas-solid flow in pneumatic conveying.

3.2. Model Equations and Analysis of the Simulated Profiles

From the models available, the equations proposed by Arastoopour and Gidaspow (1979), given by Eqs. (1), (2), (9) and (10), has been widely applied to simulate pneumatic conveyors (Rocha, 1988, Campanha, 1987) and was chosen to be simulated in this work. In this model, a fluid-wall friction force is considered in the mixture momentum balance (Eq. 9), but the solid-wall friction force is neglected. The pressure gradient term appears only in the momentum balance for the mixture, while the momentum balance for the solid phase includes the contribution of a relative velocity between the phases, a drag force and a gravitational force acting on the solids. The particles are assumed to be uniform in size, shape and density, the fluid is incompressible and the particulate phase is diluted and uniformly disbrituted over the gas phase.

For solving the equations, it was necessary to estimate the gas-wall friction force, F_f and the drag force, F_d. F_f was estimated using Eq. (13), and the friction coefficient, f_f, was calculated using the Blasius equation for smooth tubes (Bird et al., 2002), because most of experimental data obtained in our laboratories satisfied this condition. F_d was estimated from Eqs. (15) and (16), and the standard drag coefficient, C_{ds}, was obtained from Eqs. (17) and (18). The use of the standard drag curve to estimate the drag coeficients might be questioned, since the conditions for which these equations were obtained are quite different from those in pneumatic conveying. Although a correction was introduced to consider the effect of particle population in the transport tube, there are other variables which were not considered, such as the turbulence intensity in the fluid phase, the deceleration provoked by particle-particle and particle-wall collisions, and even the effect of a particle size distribution. However, the use of these equations are widespread and very few specific correlations for gas-solid turbulent flow are available in the literature, most of them obtained for conditions very different from those which will be analysed here. So this procedure was adopted for a first analysis of the model.

The simulations were carried out considering initially the conveying of spherical glass particles of particle diameter d_p=1.10 mm and density of 2,500 kg/m^3. The operational conditions and particle characteristics used as input values for the simulations were obtained from the experiments conducted by Ferreira (1996) and are given in Table (3).

The physical properties for the air were estimated at the mean temperature of the experiments. The set of equations was solved by Lourenço (2002) using a 4th order Runge-Kutta algorithm (Press et al., 1996), for different conditions of gas and solid flow rates. The integrations were performed backwards, with initial values of P and ε at z=L obtained from the measured values reported by Ferreira (1996) at fully developed conditions. The author measured the voidage in a 1.2 m long trap located at the non-acceleration section of the pipe using two quick closing electromagnetic valves. The values of v_f and v_s were obtained by applying the continuity equations at the fully developed region, which leads to:

$$W_f = \frac{v_f}{\rho_f A \varepsilon} \tag{21}$$

$$W_s = \frac{v_s}{\rho_s A(1-\varepsilon)} \tag{22}$$

where W_f and W_s are respectively the air and solid flow rates, and A is the cross-section area of the transport tube. Note that this approach avoids the use of arbitrary values as initial conditions, since there are no measured values at the position z=0.

Table 3. Input values for the simulations.

Variable	Value	Accuracy	Observations
Tube diameter (m)	0.0534	±0.5 mm	Galvanized iron
Tube lenght (m)	2.88	±0.5 mm	-
Solid flow rates (kg/s)	0.081-0.139	±3%	Experimental range
Air flow rates (m^3/s)	1.499-2.799	±0,8%	Experimental range

Typical profiles are shown in Fig. (1). In this simulation, the initial values adopted at z=L were v_f=19.5 m/s; v_s=7.01 m/s; P=451 Pa and ε=0.9968.

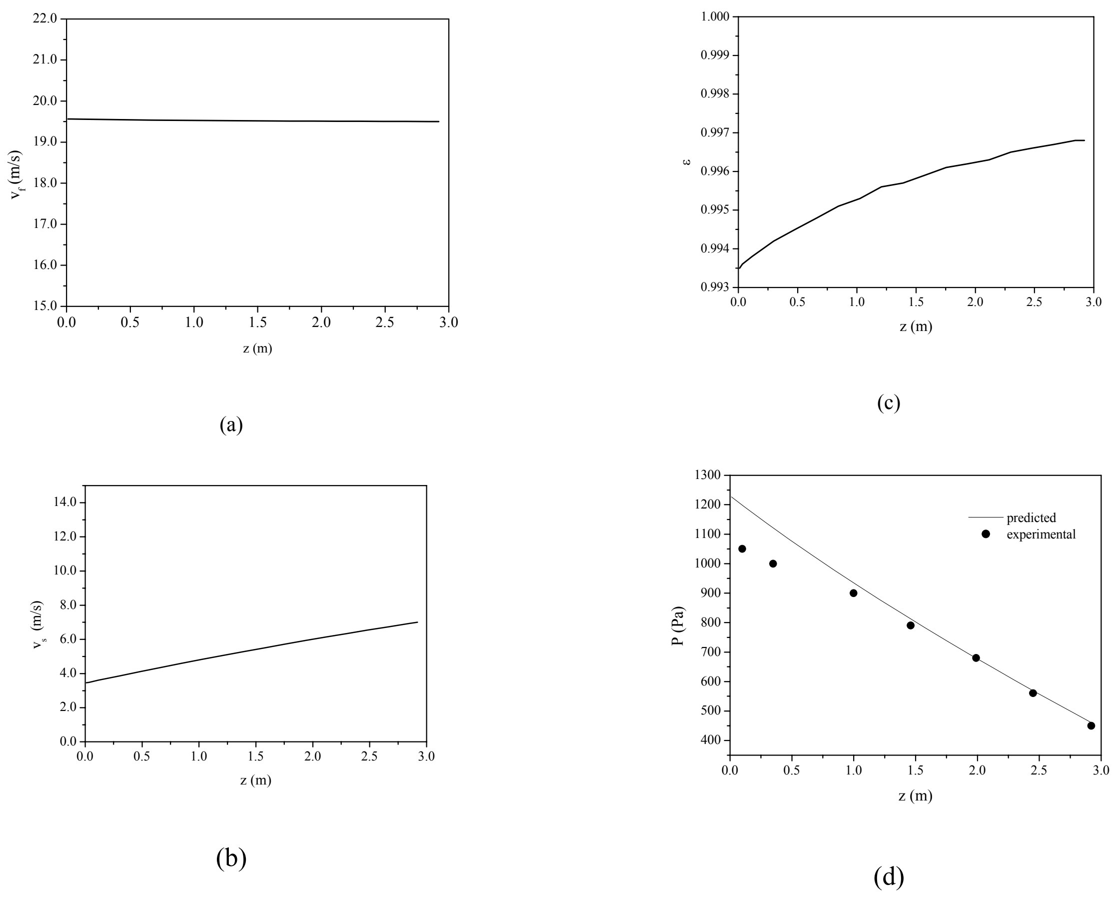

Figure 1. Graphs of (a) fluid velocity, (b) particle velocity, (c) voidage and (d) pressure as functions of axial position, glass spheres, d_p=1.10 mm, W_s=0.124 kg/s; W_f=0.0414 kg/s; L=2.88 m and D_t=53.4 mm.

The results show consistent qualitative behaviors for all the variables. The solids velocity decreases linearly from the initial value, until reaching a value of $v_s \cong 3.00$ m/s at z=0. The voidage profiles decreases smoothly from the initial value of 0.9968 at z=L to 0.9935 at z=0, while P decreases consistently as the axial distance is increased. The air velocity varied from 19.56 to 19.50 m/s, which is a practically constant value, considering the expected accuracy of an experimental measurement. The small variation of v_f values in the whole tube length is probably because the mass of air into the tube is much larger than the mass of particles, so the air velocity is practically unaffected by the transfer of momentum to the solids. The experimental pressure profile obtained by Ferreira (1996) and shown in Fig. (1d) for comparison indicates that the simulated profile agrees very well with the experimental. The large deviations are observed at the entrance region, but even there, they were always lower than 8%. Such good agreements for the pressure profiles were obtained always an experimental value was adopted as the initial value of z=L.

For flow inside tubes, the development of an accelerating region, caused by the wall-shear effects is well known (Dzido et al., 2002). The entrance length is characterized by the presence of velocities and concentration gradients, and by a non-linear variation of the pressures with the axial distance, since in this region the particles are being accelerated by the fluid. Inspection of Fig. (1d) shows that a linear pressure profile can be observed from $z\cong1.5$ m. Ferreira (1996) reported that, for the range of experimental conditions investigated, it was possible to identify a linear dependence of the pressures on the axial distance at the positions located between z=0.595 and 0.830 m. So the entrance length obtained from the simulated pressure profile is reasonably close to the experimental value, considering the uncertainties involved in experimental measurement.

An aspect to be noted is the extremely small variation of the voidage over the tube length, from 0.9935 to 0.9968. For voidage measurements using the trap valves technique, Ferreira (1996) estimated the measurement accuracy as being ±0.15%. In spite of being a very small number, for the high dilute conditions of pneumatic conveying, it is significant, since the whole variation depicted in Fig. (1c) is practically in the range of experimental uncertainty. The value of v_s predicted at z=0 (≈3.0 m/s) is also worthy note. For the most common solid feeding systems, the solids are introduced in the transport tube from the rest and such a high velocity at the tube entrance is most improbable.

According to Lourenço (2002), similar behaviors to those observed in Fig. (1) were obtained for the other conditions simulated, which included 12 runs in the range of conditions indicated in Table (3). The author reports however that the profiles are strongly dependent on the initial values adopted in the numerical integration, and different numerical solutions can be obtained for a single set of operational conditions depending on the initial values.

To check the model versatility for other kind of particles, some simulations were performed varying the particle diameter and density, by choosing arbitrary values of d_p and ρ_p, keeping the same operational conditions of Fig. (1). The profiles of P, v_s and ε are shown in Fig. (2a), (2b) and (2c), for values of d_p from 0.37 to 3.3 mm. The profile of v_f is not shown because it was not affected significantly by the variation on the particle diameter.

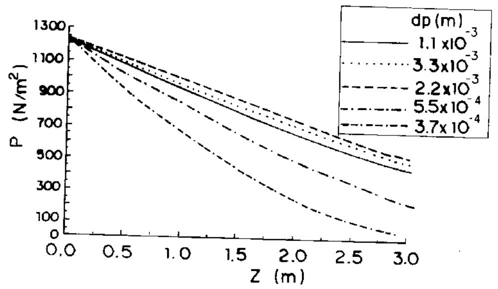

(a)

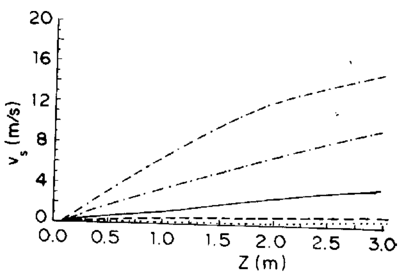

(b)

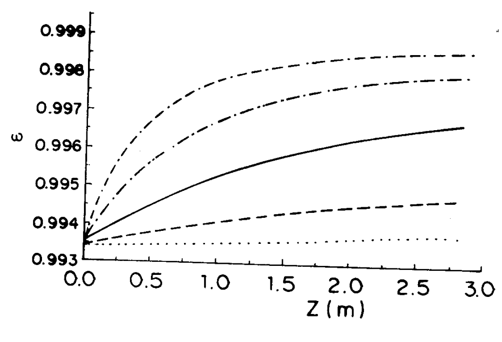

(c)

Figure 2. Graphs of (a) particle velocity, (b) voidage and (c) pressure as functions of axial position, glass spheres, W_s=0.124 kg/s; W_f=0.0414 kg/s; L=2.88 m and D_t=53.4 mm.

An increase of static pressures is expected as d_p increases, because at a constant solid flow rate, the larger particle volumes result in higher drag and gravitational forces. This tendency appears clearly in Fig. (2a), but it is worth note that the increase in the pressures is much more accentuated for the smallest particle diameters (0.37 and 0.55 mm). Increasing d_p from 1.1 to 2.2 mm caused a variation within the experimental uncertainty in the pressures and a further increase of d_p to 3.3 mm practically did not affect the pressures. Figure (2b) shows that the solids velocity decreases as the particle diameter is increased, but for the largest d_p (2.2 and 3.3 mm), v_s stays practically constant and near to zero, indicating that there is no solids transport at these conditions. The pressure profiles shown in Fig. (2a) for these largest particle diameters are in fact due to the fluid flow alone, thus explaining their small dependence on the particle diameter variation. The voidage profiles showed in Fig. (2c) present a consistent behavior, with the voidages decreasing as the particle diameter increases, but again the variations are much more accentuated for the smallest particles. The variation of particle density in a range from 834 to 7509 kg/m^3 provided similar profiles to those presented in Fig. (2), but for concision they will not be reproduced here (details can be found in Lourenço, 2002). The results obtained by varying d_p and ρ_p indicate that the model equations can not be applied for a large range of conditions without a careful analysis of its performance and prior validation.

In experimental systems, the measurement of static pressures can be easily performed and there is a great number of pressure gradient data available in the literature. Graphs of pressure gradients versus air velocity are important because they allow the knowledge of how the system responds to variations in the air and solid flow rates, and also provides information concerning the conveying regime and transition from dense to dilute flow (Marcus et al., 1990). The pressure gradients can be obtained from the slope of the curves of P versus z, calculated at the region of linear behavior (full-developed flow). In order to validate the model, the pressure gradients predicted by the model are compared to experimental results reported by Narimatsu (2000). The results are shown in Fig. (3).

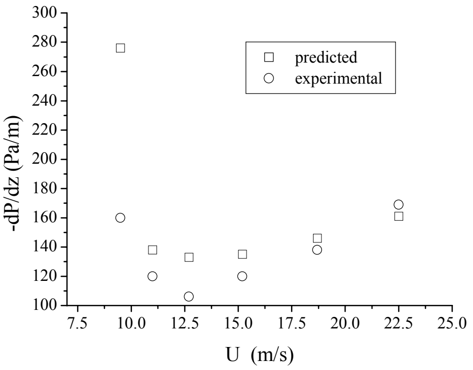

Figure 3. Experimental and predicted pressure gradients versus air velocity in the transport tube, glass spheres, d_p=1.00 mm; W_s=0.041 kg/s (experimental data from Narimatsu, 2000).

It can be seen that as the air velocity is reduced from the highest values, the pressure gradient decreases until reaching a minimum value. From this point on, a further reducing of the air velocity causes an increase in the pressure gradients. According to Marcus et al. (1990), the change in the curve behavior is caused by the increasing in the solids holdup observed as the air velocity is reduced at a constant solid flow rate. The air velocity at the point of minimum gradient, U_{min}, corresponds to the transition velocity between the dilute conveying, located at the right of the curve and dense-phase conveying, located at the left region.

The agreement between the simulated and experimental values is quite good, particularly at the greatest values of U. The deviations increase as the air velocity is reduced, and at air velocities lower than 20.0 m/s, the model predictions always underestimate the pressure gradients. At the greatest air velocities, the voidages increase and the fluid dynamic behavior is affected mainly by the fluid characteristics. When the air velocity is reduced, the contribution of gravitational and drag forces becomes significant and the model do not perform as well. The great deviation observed at U=9.41 m/s is not surprising because it corresponds to a typical point of dense-phase transport, so the dilute-phase model adopted here is not to be applied at this condition. It is interesting to note that the simulations allow a good prediction for U_{min}, which can be considered as very positive result as far a control application is concerned.

Additional simulations were performed for glass spheres of diameters equal to 1.00; 2.05; 2.85 and 3.68 mm, at similar conditions of air velocity and solid flow rates. The results are compared to experimental data reported by Narimatsu (2000), as depicted in Fig. (4). The predicted pressure gradients show a good agreement with the experimental values, with deviations in the range of experimental error. Such results confirm that at dilute conditions, the fluid dynamic behavior is defined by the fluid phase behavior and the particle characteristics do not affect the results significantly.

A comparison between predicted and experimental pressure gradients obtained for particles of different densities is shown in Fig. (5). It can be noted that, in spite of the underestimated predicted values for both particle densities, the deviations are relatively small, particularly at dilute conditions and tend to increase as the air velocity is reduced and the dense-phase transport regime is reached. The experimental curve of dP/dz versus z for the glass spheres indicates that U_{min} is located in a range between 18.0 and 21.0 m/s. In the simulated curves, U_{min} appears in the same range, agreeing quite well with the experimental result. For the particles of smaller density, however, the simulations did not predict a transition in the regimes, which was experimentally observed between 14.0 and 16.0 m/s.

Another point to be noted is the lack of dependence of the pressure gradients on the particle density, observed both experimentally and in the simulations.

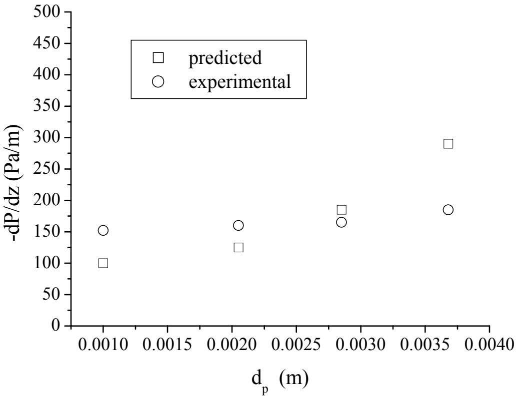

Figure 4. Experimental and predicted pressure gradients as functions of the particle diameter; U=22 m/s and W_s=0.042 kg/s.

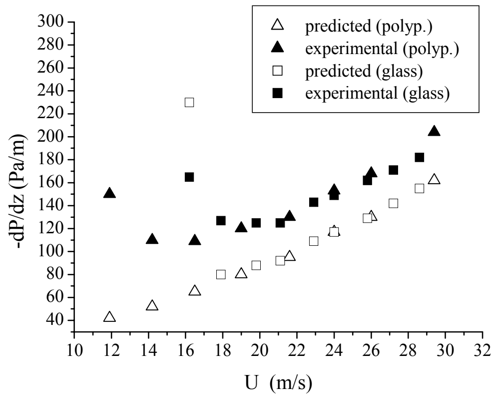

Figure 5. Predicted and experimental pressure gradients as functions of air velocity for glass spheres (ρ_p=2500 kg/m^3) and polipropylene beads (ρ_p=935 kg/m^3); d_p=3.68 mm; W_s=0.037 kg/s.

4. Conclusions

The two-fluid one-dimensional model cannot be considered a phenomenological model, essentially due to the assumption that the particulate phase can be treated as a continuous fluid. The physical analysis of the model indicates that the requirement of a meaningful control volume $\Delta V \rightarrow 0$ is not accomplished by a gas-solid mixture. Even so, the two fluid model provided good predictions of some macrosocopic fluid dynamic variables, particularly at dilute-phase conditions. This possibly occurs because: (i) the empirical constitutive equations themselves perform as fitting parameters that in some way correct the model deficiencies, and (ii) at very diluted conditions the fluid-dynamic properties are defined, actually, by the fluid phase, and the presence of solids has little effect on the flow behavior.

The variation of v_f, v_s, ε and P along the transport tube could be obtained by backwards numerical integration of the continuity and momentum equations proposed by Arastoopour and Gidaspow (1979). The profiles were observed to be strongly dependent on the variables initial values. A good agreement between the predicted and experimental pressure profiles was obtained only when the initial values were estimated based on experimental measurements. The model also provided good predictions of pressure gradients and allowed reasonable estimates of the entrance length and of the minimum air velocity in which occurs the transition between dense and dilute regimes. One may conclude that, in spite of its deficiencies, the two-fluid model can be considered a simple and effective model for prediction of controlable variables in a further automation of a drying process, but it still depends a lot on experimental information.

5. Acknowledgements

The authors thank PRONEX/CNPq for the financial assistance.

6. Reference List

Arastoopour, H. and Gidaspow, D., 1979, “Vertical Pneumatic Conveying Using Four Hydrodynamic Models”, Ind. Eng. Chem. Fund., Vol. 18, no. 2, pp. 123-130.

Bear, J., 1972, “Fluids in Porous Media”, American Elsevier Publ. Co., New York, USA, 764 p.

Berker, R., 1963, “Intégration des Équations du Movement d´un Fluid Visquex Incompressible”, Handbuch der Physik (Flügge, S., Ed.), Vol. VIII, Spring-Verlog, Berlin, 384 p.

Bird, R.B., Stewart, W.E. and Ligthfoot, E.N., 2002, “Transport Phenomena”, 2nd ed., John Wiley & Sons, 895 p.

Campanha, J.R., 1987, “Modelagem e Simulação de Secadores Pneumáticos Verticais”, Dissertação de Mestrado, FEQ/UNICAMP, 131 p.

Capes, C.E. and Nakamura, K., 1973, “Vertical Pneumatic Conveying: an Experimental Study with Particle in the Intermediate and Turbulent Flow Regimes”, Can. J. Chem. Eng., Vol. 51, no. 3, pp. 31-38.

Clift, R., Grace, J.R. and Weber, M.E., 1979, “Bubbles, Drops and Particles”, Academic Press, New York, 380 p.

Deich, M.E., 1974, “Critical Conditions in Two-phase Flows with a Continuous Vapor or Gas Phase”, High Temperature, Vol. 12, no. 2, pp. 299-307.

Drew, D.A., 1983, “Mathematical Modeling of Two-Phase Flow”, Ann. Rev. Fluid Mechan., Vol. 15, pp. 261-291.

Dzido, G., Palica, M. and Raczek, J., 2002, “Investigations of the Acceleration Region in the Vertical Pneumatic Conveying”, Powder Technol., Vol. 127, pp. 99-106.

Enwald, H. and Almstedt, A.E., 1999, “Fluid Dynamics of a Pressurized Fluidized Bed: Comparison Between Numerical Solutions from Two-fluid Models and Experimental Results”, Chem. Eng. Sci., Vol. 54, pp. 329-342.

Ferreira, M.C., 1996, “Desenvolvimento de um Leito Pneumático com Alimentador Tipo Jorro”, Tese de Doutorado, PPG-EQ/UFSCar, 194 p.

Gidaspow, D., 1994, “Multiphase Flow and Fluidization – Continuum and Kinetic Theory Descriptions”, Academic Press, 467 p.

Graham, D.I. and Moyeed, R.A., 2002, “How Many Particles for my Lagrangian Simulations?” , Powder Technol., Vol. 125, pp. 179-186.

Haider, A. and Levenspiel, O., 1989, “Drag Coefficient and Terminal Velocity of Spherical and Non-Spherical Particles”, Powder Technol., Vol. 58, pp. 63-70.

Hoomans, B.P.B., Kuipers, J.A.M., Briels, W.J. and Van Swaaij, W.P.M., 1996, “Discrete Particle Simulation of Bubble and Slug Formation in a Two-Dimensional Gas-Fluidized Bed; a Hard Sphere Approach”, Chem. Eng. Sci.,Vol. 51, pp. 99-108.

Hubber, N. and Sommerfield, M., 1998, “Modelling and Numerical Calculation of Dilute-Phase Pneumatic Conveying in Pipe Systems”, Powder Technol., Vol. 99, pp. 90-101.

Khan, A.R. and Richardson, J.F., 1987, ‘The Resistance to Motion of Solid Sphere in a Fluid”, Chem. Eng. Comm., Vol. 62, pp. 135-150.

Kuipers, J.A.M., Van Duin, K.J., Van Beckum, F.P.H. and Van Swaij, W.P.M., 1992, “A Numerical Model of Gas-Fluidized Beds”, Chem. Eng. Sci., Vol. 47, no. 8, pp. 1913-1924.

Lee, S.L. and Durst, F., 1982,”On the Motion of Particles in Turbulent Duct Flows”, Int. J. Multiphase Flow, Vol. 8, no. 2, pp. 125-146.

Levy, A., 2000, “Two-fluid Approach for Plug Flow Simulations in Horizontal Pneumatic Conveying”, Powder Technol., Vol. 112, pp. 263-272.

Littman, H., Morgan, M.H., Paccione, J.D., Jovanovic, S.Dj. and Grbavcic, Z.B., 1993, “Modelling and Measuremnte of the Effective Drag Coefficient in Deceleranting and Non-accelerating Turbulent Gas-Solids Dilute Phase Flow of Large Particles in a Vertical Transport Pipe”, Powder Technol., Vol. 77, pp. 267-283.

Lourenço, C.A., 2002, “Análise da Aplicação do Modelo Bifásico Unidimensional para a Modelagem Matemática do Comportamento Fluidodinâmico do Transporte Pneumático Vertical”, Dissertação de Mestrado, PPG-EQ/UFSCar, 97 p.

Marcus, R.D., Leung, L.S., Klinzing, G.E. and Risk, F., 1990, “Pneumatic Conveying of Solids: A Theoretical and Practical Approach”, Powder Technology Series, St. Edmundsbury Press, 575 p.

Narimatsu, C.P., 2000, “Transporte Pneumático em Fases Densa e Diluída – Influência da Densidade e do Diâmetro das Partículas no Comportamento Fluidodinâmico”, Dissertação de Mestrado, PPG-EQ/UFSCar, São Carlos-SP, 84 p.

Niewland, J.J., Veenendaal, M.L. Kuipers, J.A.M. and Van Swaij, P.M., 1996, “Bubble Formation at a Single Orifice in Gas Fluidised Beds”, Chem. Eng. Sci., Vol. 51, pp. 4087-4102.

Ouyang, J. and Li, J., 1999, “Discrete Simulations of Heterogeneous Structure and Dynamic Behavior in Gas-Solid Fluidization”, Chem. Eng. Sci., Vol. 54, pp. 5427-5440.

Press, H., Teukolsky, A., Vetterling, W.T. and Flannery, B.P., 1994, “Numerical Recipes in Fortran”, Cambridge University Press, 963 p.

Richardson, J.F. and Zaki, W.N., 1954, “Sedimentation and Fluidization- Part I”, Trans. Inst. Chem. Engs., Vol. 32, pp. 33-53.

Rocha, S.C.S., 1988, “Contribuição ao Estudo da Secagem Pneumática Vertical: Simulação e Influência do Coeficiente de Transferência de Calor Gás-Partícula”, Tese de Doutorado, EPUSP, 258 p.

Rowe, P.N., 1961, “Drag Forces in a Hydraulic Model of Fluidized Bed, part II”, Trans. Inst. Chem. Engs., Vol. 39, pp. 175-180.

Soo, S.L., 1967, “Fluid Dynamics of Multiphase Systems”, Walthan, Massachussets, Blaisdell Pub. Co.

Telles, A.S. and Massarani, G., 1992, “Escoamento de Soluções e Suspensões Não-Newtonianas em Dutos “, Anais do XX ENEMP, pp. 27-33, São Carlos, Brasil.